Project	**IEEE 802.16 Broadband Wireless Access Working Group**
Title	**Proposed System Impairment Models**
Date Submitted	**2000-02-29**

Source	David Falconer Dept. of Systems and Computer Engineering Carleton University Ottawa, Ont., Canada K1S 5B6	Voice: +1 613 520 5722 Fax: +1 613 520 5727 Email: ddf@sce.carleton.ca
	Tom Kolze Broadcom Corp. 16037 South 18th Place Phoenix, AZ 85048, USA	Voice: +1 480 460 2894 Fax: +1 480 460 2292 Email: tkolze@getnet.com
	Yigal Leiba BreezeCOM Ltd. Atidim Technology Park Bldg. 1 P.O. Box 13139 Tel Aviv 61131, Israel	Voice: +972 3 6456254/6262 Fax: +972 3 6456290/6222 Email: igall@breezecom.co.il
	John Liebetreu SiCOM Inc. 7585 E. Redfield Rd. Scottsdale, AZ 85260, USA	Voice: +1 480 607 4830 Fax: +1 480 607 4806 Email: john@sicom.com

Re:	Response to IEEE 802.16 PHY Task Group Call for Contributions on Modelling Issues, Jan. 13, 2000, in particular the call for models of power amplifier nonlinearity, phase noise and channel multipath.

Abstract	**We propose models, with appropriate parameters, of power amplifier nonlinearity, phase noise and multipath channel impulse response, against which PHY layer solutions may be tested.**

Purpose	Aid in the PHY Task Group's preparation of a detailed evaluation table for performance of PHY layer air interface proposals.

Proposed System Impairment Models

David Falconer, Tom Kolze, Yigal Leiba and John Liebetreu

1. Introduction – Sources of Performance Degradation Considered

In this contribution we propose models for the following system impairments:

- Phase noise
- Power amplifier nonlinearities
- Multipath channel response.

These models are offered for the purpose of performance evaluation of air interface PHY layer proposals.

2. Phase Noise Model

The purpose of the phase noise model is to facilitate *comparison* of 802.16.1 physical layer proposals' sensitivity to phase noise. This model *is not* proposed as an interface specification, and it is not proposed as an element in a simulation or analysis attempting to predict a precise performance for a proposal.

The model is describing the composite phase noise on the signal input to the demodulator in the receiver (after downconversion). Phase noise is introduced by 1) the local oscillator signal feeding the mixer in the transmitter upconverter (at the base station for the downstream and at the CPE for the upstream) and 2) by the local oscillator feeding the mixer in the receiver downconverter. Phase noise is also present on the modulated signal input to the transmitter upconverter (for upconversion to the transmission radio frequency of between 10 GHz to 66 GHz in 802.16.1), but this phase noise is expected to be insignificant compared to that introduced in the upconversion and downconversion units.

Additional phase noise may be introduced within the demodulator; in particular, thermal noise at the demodulator input may contribute phase noise to any carrier reference signals developed within the demodulator. This demodulator-introduced phase noise is *not included* in the model.

The phase noise model itself consists of a mask of the Single Sideband (SSB) phase noise Power Spectral Density (PSD), in units of dBc/Hz plotted against log10 of the offset from the carrier frequency. No discrete spurious are included in this simplistic model.

The modeled shape of the phase noise SSB PSD is characterized by four parameters, which are to be selected and varied in parametric performance analyses of the waveforms proposed for the 802.16.1 standard. The model assumes a synthesizer with a phase locked loop (PLL) is used to generate the conversion mixer frequencies. The four parameters of the model are:

- F_{xtal}--the corner frequency where the crystal oscillator $1/f^2$ slope drives below the floor of the synthesizer's PLL;
- L_{loop}-- the floor of the synthesizer PLL in the passband of the loop (i.e., phase detector noise);
- F_{loop}-- the corner frequency of the synthesizer PLL;
- L_{floor}-- the far-out floor of the converters' local oscillators (out to 100 MHz).

The SSB phase noise PSD, and the four parameters, are illustrated in **Figure P1**. (Recall, the model is depicting the composite phase noise presented to the demodulator, and it is describing the Single Sideband phase noise.

The total integrated phase noise, in units of radians squared, is the integral of the mask from 0 Hz offset frequency to infinite offset frequency, and then multiplied by two to account for the other sideband.)

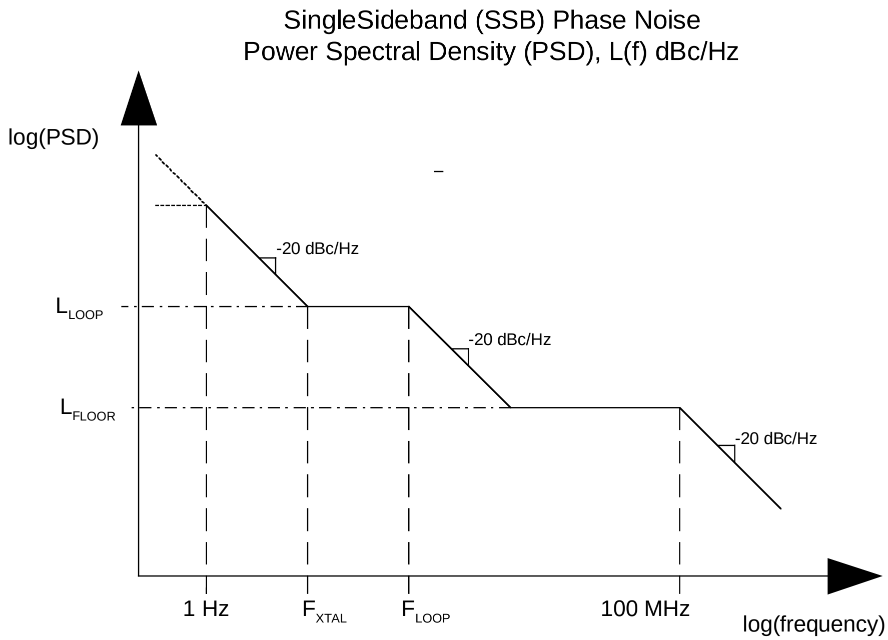

Figure P1. Parameterized Phase Noise Model for Comparing Physical Layer Proposals' Performance Sensitivity to Phase Noise.

Instead of attempting to derive a reality-driven but highly specific, implementation-dependent SSB phase noise PSD, rather a generic and easy-to-use model has been developed. This model is believed to capture the essential characteristics of the phase noise occurring in actual applications, especially considering the flexibility in the choices of the model parameters. However, the complexity trade-offs and the vast array of implementation choices in designing the up- and downconverters makes it difficult to settle on a reality-based phase noise model without a full airing of the design and complexity of the choices available.

(Such an effort must be undertaken if an interface specification on phase noise is to be levied. A compromise solution may involve more than one mask—perhaps a high fidelity mask and a low fidelity mask, as an example. As another example, a model scaling one or more of the parameters as a function of radio frequency may be useful since there are almost three octaves of transmission frequency.)

It is conceded that in some respects the model does not provide a rigorously realistic shape. In particular, the PSD mask behavior or shape at the close-in (low offset frequencies) of the crystal-oscillator-dominated portion of the model is set at a slope of –20 dBc/Hz, until reaching to within 1 Hz of the carrier frequency. At 1 Hz, the mask may be continued at –20 dBc/Hz, or flattened to a constant density for < 1 Hz offsets. For purposes of computing a phase noise power, it may be useful to invoke the flattened mask, and for simulation purposes, continuing the –20 dBc/Hz slope may prove be more easy to apply. For simulation durations significantly less than 1 second there should be no discernible impact in choosing one method for analysis and the other for simulation. Whichever approach is taken, the choice should be reported along with the parameter values chosen.

In reality, the close-in slope is likely steeper than the –20 dBc/Hz in the model, such as 1/f, and the mask continues rising indefinitely for closer-in offset frequencies. Although not strictly holding to reality, the selected model is believed to provide a basis for meaningful comparison of competing physical layer waveforms since the predominant characteristics are included. The selected model is readily amenable to simulation and analysis owing to 1) the –20 dBc/Hz slopes (which correspond to integrated white noise), and 2) the zero at 1 Hz—i.e., the flattening of the PSD at low offset frequencies, and the pole at 100 MHz, which together provide finite power in integrating the area under the PSD.

Thus, while a strictly reality-driven model is not proposed, such a model would require much meaningful debate, would be much more difficult to simulate and analyze, and would likely not provide any substantial benefits in a relative assessment of phase noise sensitivity for competing physical layer proposals.

3. Power Amplifier Model

We recommend the well-known "Saleh model" as a comparison baseline to use in characterizing the effect of the power amplifier in a broadband wireless access system; as the baseline model, it will serve as a reference point for comparison with other power amplifier models. The Saleh modeling technique, developed and discussed in [Sal81], uses simple two-parameter functions to model the amplitude-to-phase (AM to PM) and amplitude-to-amplitude (AM-to-AM) characteristics of nonlinear amplifiers. In particular, the models described in [Sal81] specify the behavior of traveling-wave tube amplifiers (TWTAs), although appropriate selections for the amplitude and phase coefficients (α's and β's) described below provide a suitable model for solid state amplifiers as well. Saleh's models for TWTAs are shown to accurately match actual measured data. A brief summary of the technique is included here for purposes of illustration.

Let the input signal be

$$x(t)=r(t)\cos[\omega_0 t+\psi(t)],$$

where ω_0 is the carrier frequency, and $r(t)$ and $\psi(t)$ are the modulated envelope and phase, respectively.

The output of the nonlinear amplifier is written

$$y(t)=A[r(t)]\cos\{\omega_0 t+\psi(t)+\Phi(r(t))\}$$

where $A(r)$ is an odd function of r and represents the AM-to-AM conversion, and $\Phi(r)$ is and even function of r representing the AM-to-PM conversion.

The specific form of the two functions is:

$$A(r)=\alpha_a r/(1+\beta_a r^2)$$

$$Q(r)=\alpha_\phi r^2/(1+\beta_\phi r^2)$$

Saleh presents several sets of amplitude and phase coefficients that correspond to different TWT devices. The particular set determined from data specified by Kaye, George, and Eric [Kay72], are frequently cited in the literature. These parameters values are:

α_a= 2.1587

β_a= 1.1517

α_ϕ= 4.033

β_ϕ= 9.1040

See **Figure N1** for a plot of the amplitude-to-phase (AM to PM) and amplitude-to-amplitude (AM-to-AM) characteristics of the nonlinear amplifier with these coefficients.

A simplified model that is occasionally cited uses the following coefficients:

α_a= 2.0

β_a= 1.0

α_ϕ= 2.0

β_ϕ= 1.0

Note that the AM-to-AM parameters of the simplified model are close to the exact parameters, but the AM-to-PM parameters are quite different.

The characteristics for the simplified model are shown in **Figure N2**.

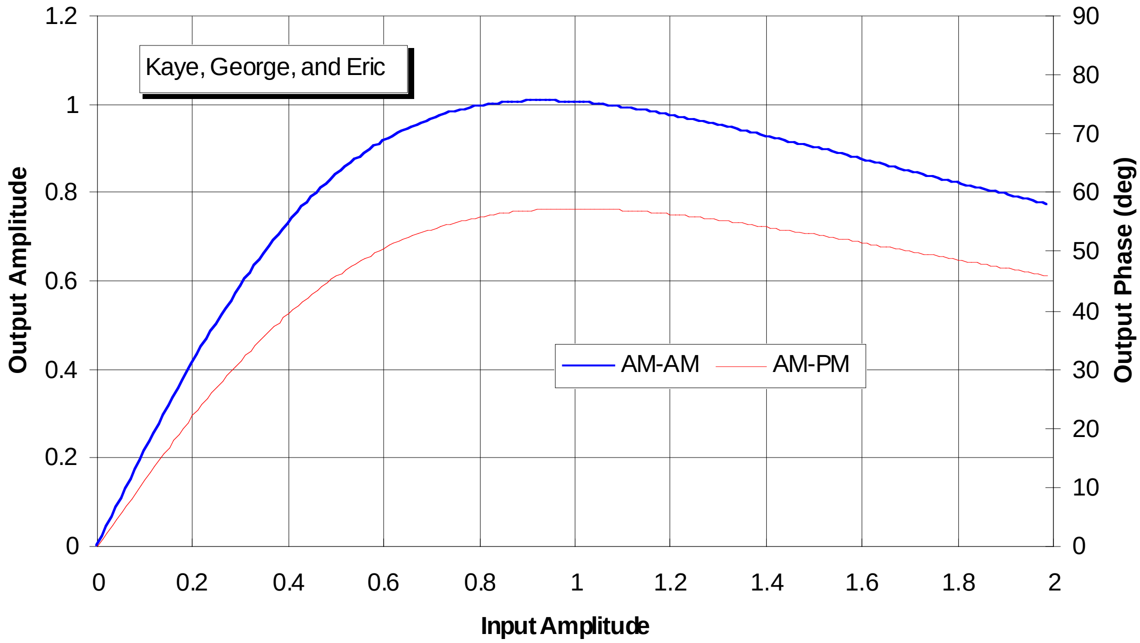

Figure N1: Plot of the AM to PM and AM to AM characteristics of the Saleh model for the coefficients that match the measurement data obtained by Kaye, George and Eric

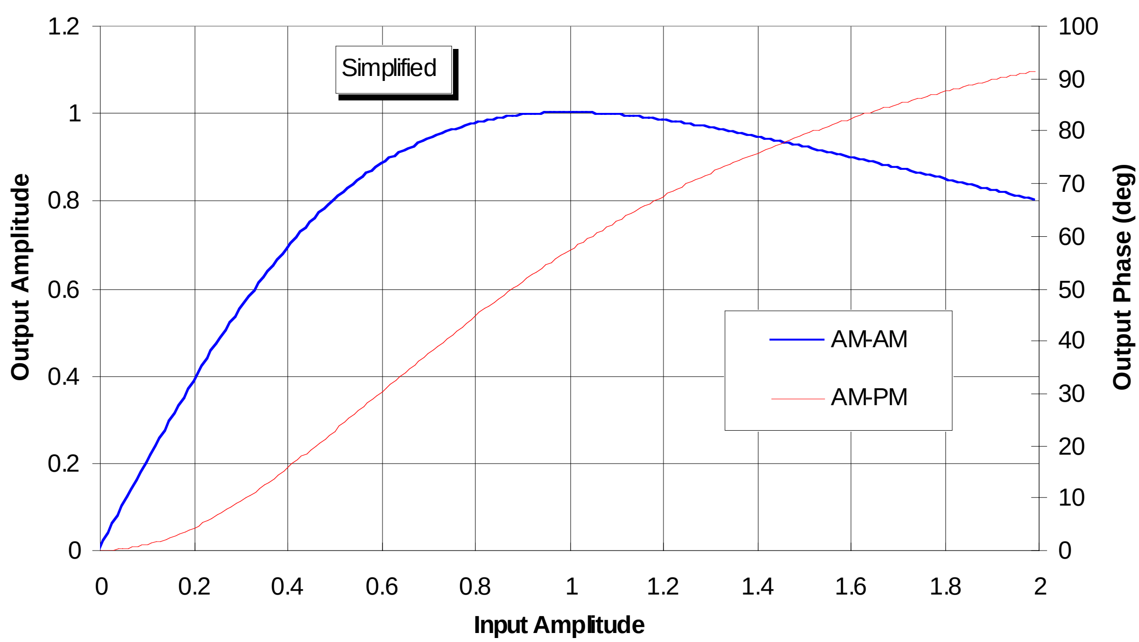

Figure N2: Plot of the AM to PM and AM to AM characteristic of the Saleh model for simplified coefficients

Another model frequently referenced in the literature is the so-called "Rapp model [Rap91]." This model is often used tp represent solid-state power amplifiers. It produces a smooth transition for the envelope characteristic as the input amplitude approaches saturation.

$Vout = Vin/(1 + (|Vin|/Vsat)^{2P})^{1/(2P)}$

where Vsat is the saturation voltage of the power amplifier and P is the smoothness factor. Curves for various values of P are plotted in **Figure N3**.

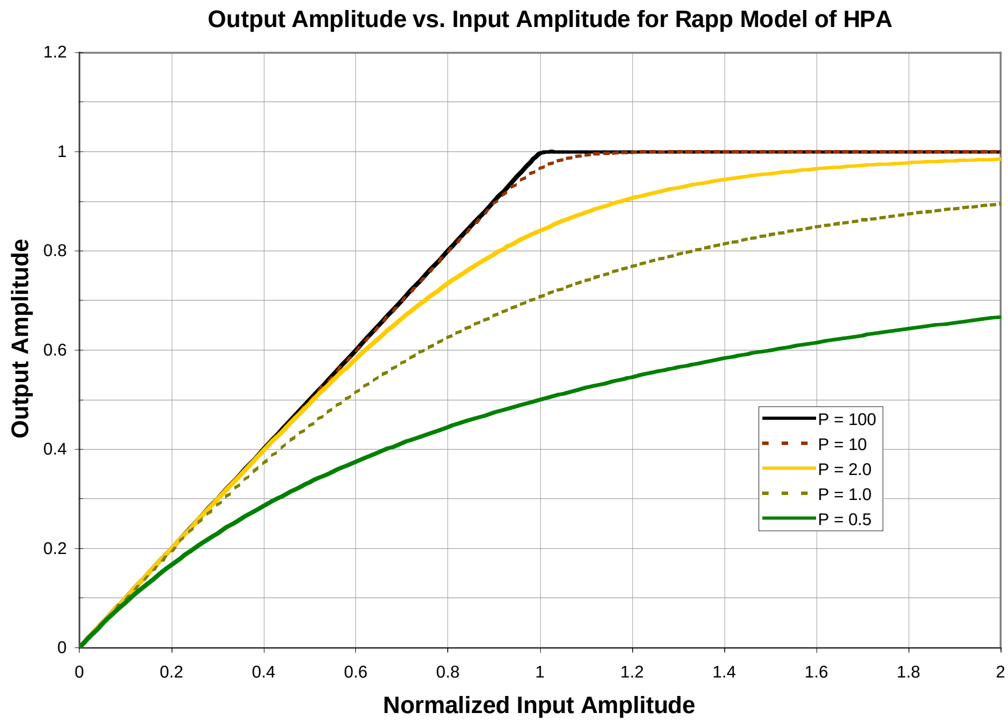

Figure N1: The AM to AM characteristic for the Rapp nonlinear power amplifier model for various smoothing parameters.

The performance metric is the lowest output power back-off, which is measured by,

$OPB = 10\log(P_{sat}/Avg(|V_{out}|^2))$

where P_{sat} is the limiting output power and $Avg(|V_{out}|^2)$ is the average amplifier output power. The Rapp model has been modified for bipolar devices in order to take into account the exponential nature of the relationship between the input and output amplitudes at low power levels [Hon97]. This modified version agrees more closely with actual measurements, particularly of intermodulation products, than the original Rapp model. Unlike the Saleh model, parameters for this modified Rapp model are not yet readily available in the literature.

4. Multipath Model

4a. Background

Broadband wireless systems of the type envisaged in the 802.16.1 functional requirements document will likely tend to be deployed with highly directive subscriber antennas in environments offering line of sight transmission. Nevertheless, an intersymbol interference impairment may occur as a result of multipath – reflections, scattering or diffraction caused by objects near the line of sight path, which are illuminated by an antenna beam. These multipath components may change with environmental conditions; for example wet leaves and flat roofs covered with water have different scattering and reflection properties from their dry counterparts.

For simplicity, we aim to propose deterministic models of multipath channel impulse responses, with variable parameters, rather than the statistical models proposed in [Fal99b]. In general a modelled complex sampled response has its time origin at t=0, and its energy (sum of squared magnitudes of its samples) is normalized to unity. Thus the modeled impulse response is of the form

$\{h(k\Delta t) \equiv h_k\}_{k=-\infty}^{\infty}$, where Δt is an appropriate sampling interval, and

$$\sum_{k=-\infty}^{\infty} |h_k|^2 = 1.$$

The use of highly directive antennas (e.g. ±1° beamwidth), at least at the subscriber's end, as well as careful placement of subscriber and base antennas to achieve LOS paths, should limit the maximum spread $|k\Delta t|$ to moderate values; e.g. ~60 ns. or less. Measurement data using directive antennas at millimeter wave frequencies supporting this hypothesis include: the Kanata data described in [Fal99b], (but not the Parkwood Hills data, for which wider antennas and non-LOS paths were prevalent), as well as data reported in [Vio88], [Pap97a], and [Xu99]. **Fig. M1** shows the four worst-case Kanata responses, obtained as deviations from the mean response, as described in [Fal99b], and sampled at 20 ns. intervals.

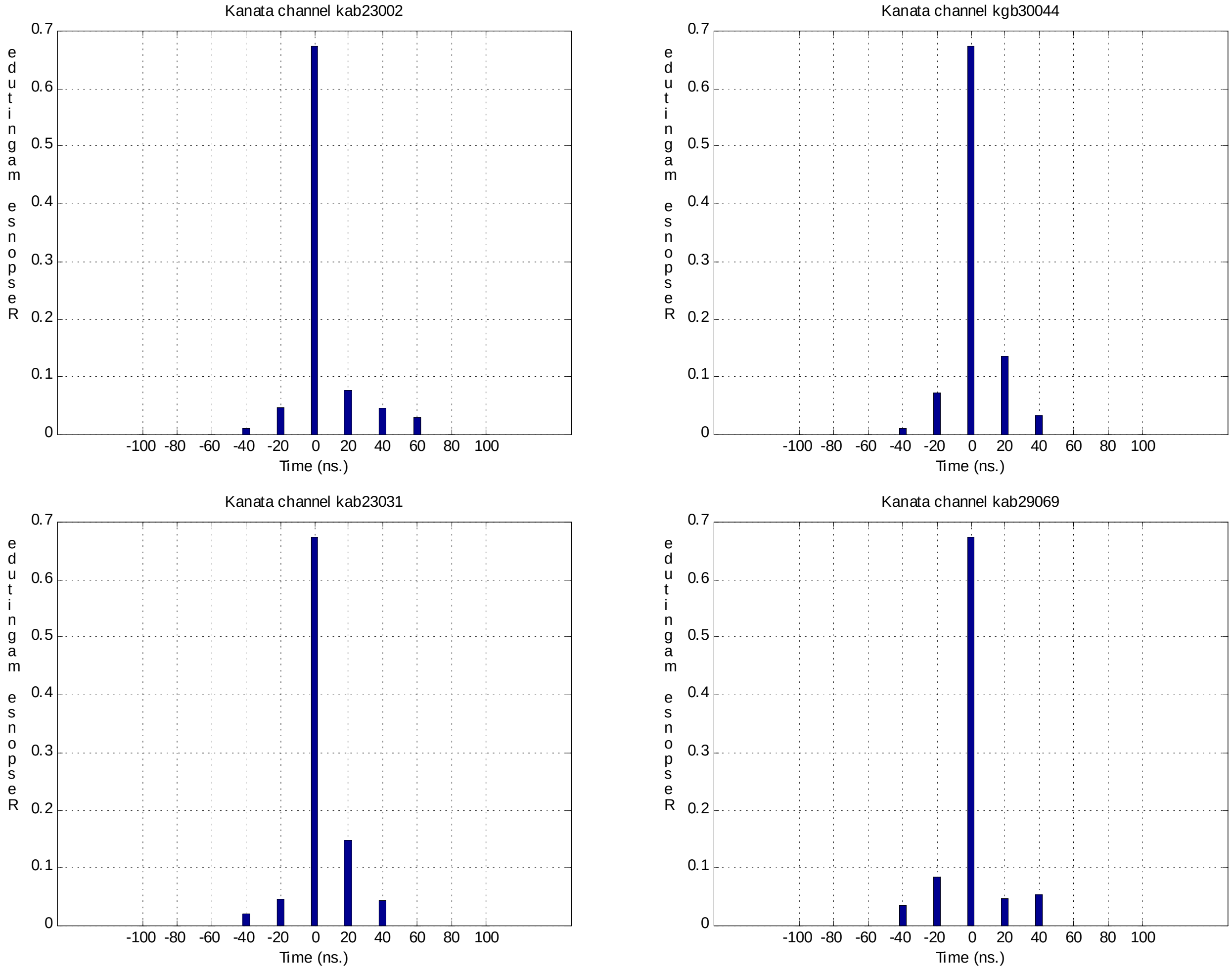

Fig. M1 The worst-case Kanata responses

Several deterministic multipath models were proposed for use in the ETSI/BRAN standards group [ETSI99]. In unnormalized form they are shown in **Fig. M2**. The same document also mentions that T1 and T2 are models based on measurements in Europe. Models G3, G4 and L7, causing more severe distortion than T1 and T2,

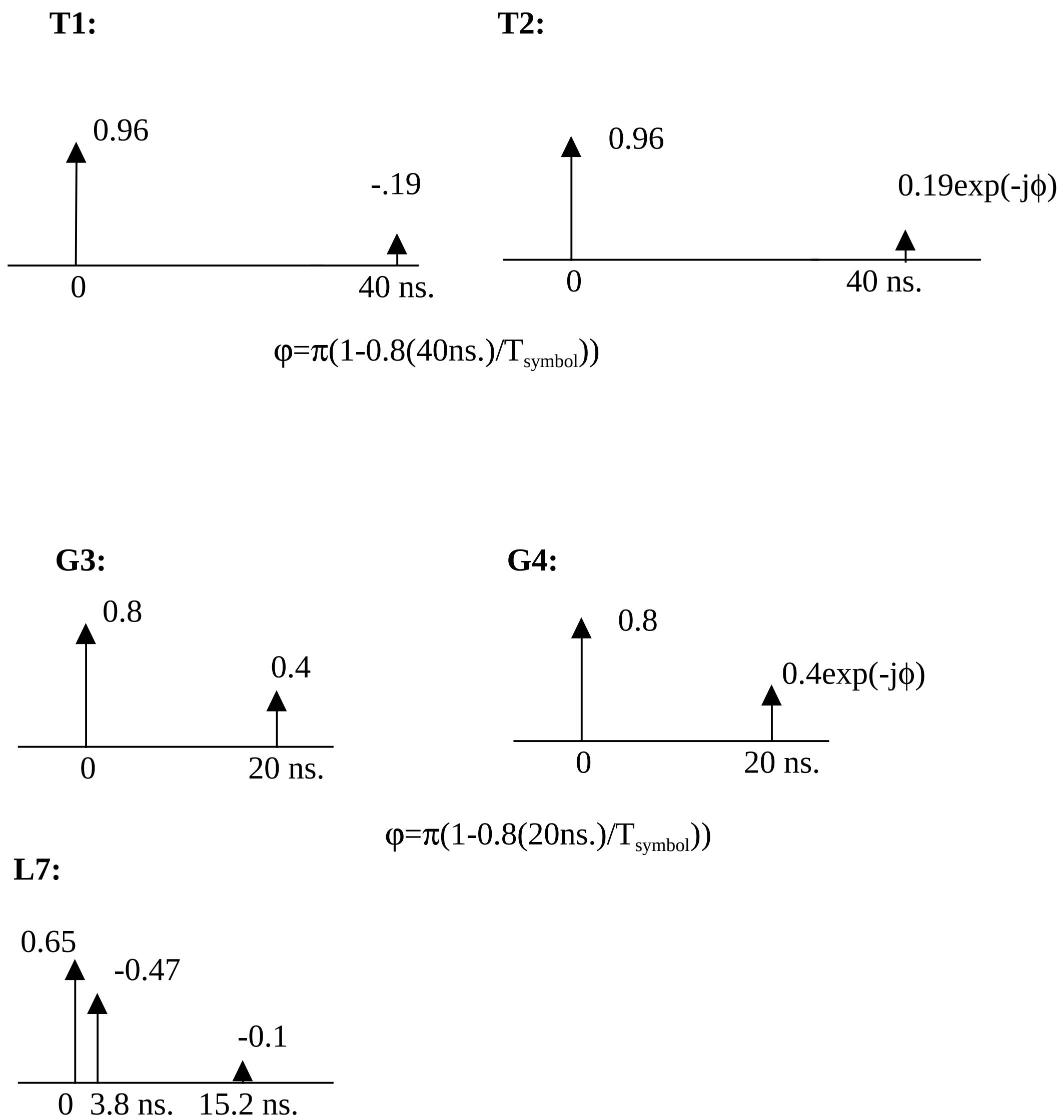

Fig. M2 Proposed ETSI/BRAN models [ETSI99]

are proposed for use in system evaluations. It is worth noting that model L7 is virtually the same as a measured "bad" impulse response described in [Pap97a], which was based on measurements in Northglen, CO. It should also be noted that L7 is approximately a two-ray model, with the first ray severely attenuated (faded). Another type of model, which has been found useful in situations with severe multipath resulting from many widely-spaced scatterers or reflectors, and relatively wide antenna beams is the exponentially decaying statistical model [Cha00], [Erc99]. It is felt that this type of model is less useful in the 802.16.1 context, and it will not be considered further.

4b The Models Proposed

The measured channel impulse responses reported in [Fal99b] included a number with significant precursors; i.e. echo components appearing before the main echo. These represented situations where the shortest radio path is attenuated relative to some slightly longer paths – perhaps due to partial attenuation or blocking of the LOS path by obstructions. For this reason our proposed models include some with precursor echoes. The models, which are shown in **Fig. M3**, are intended to be useful for evaluation of PHY solutions with bandwidths from a few MHz up to about 50 MHz. They are to be regarded as “worst case” responses for PHY evaluation purposes. All produce a higher degree of intersymbol interference than any of the measured Kanata responses in [Fal99b]. However they are all better than some of the worst Parkwood Hills responses. Because of the relatively small amount of measured data available from few locations, they represent a “best guess” as to what are typical worst case responses would be in general.

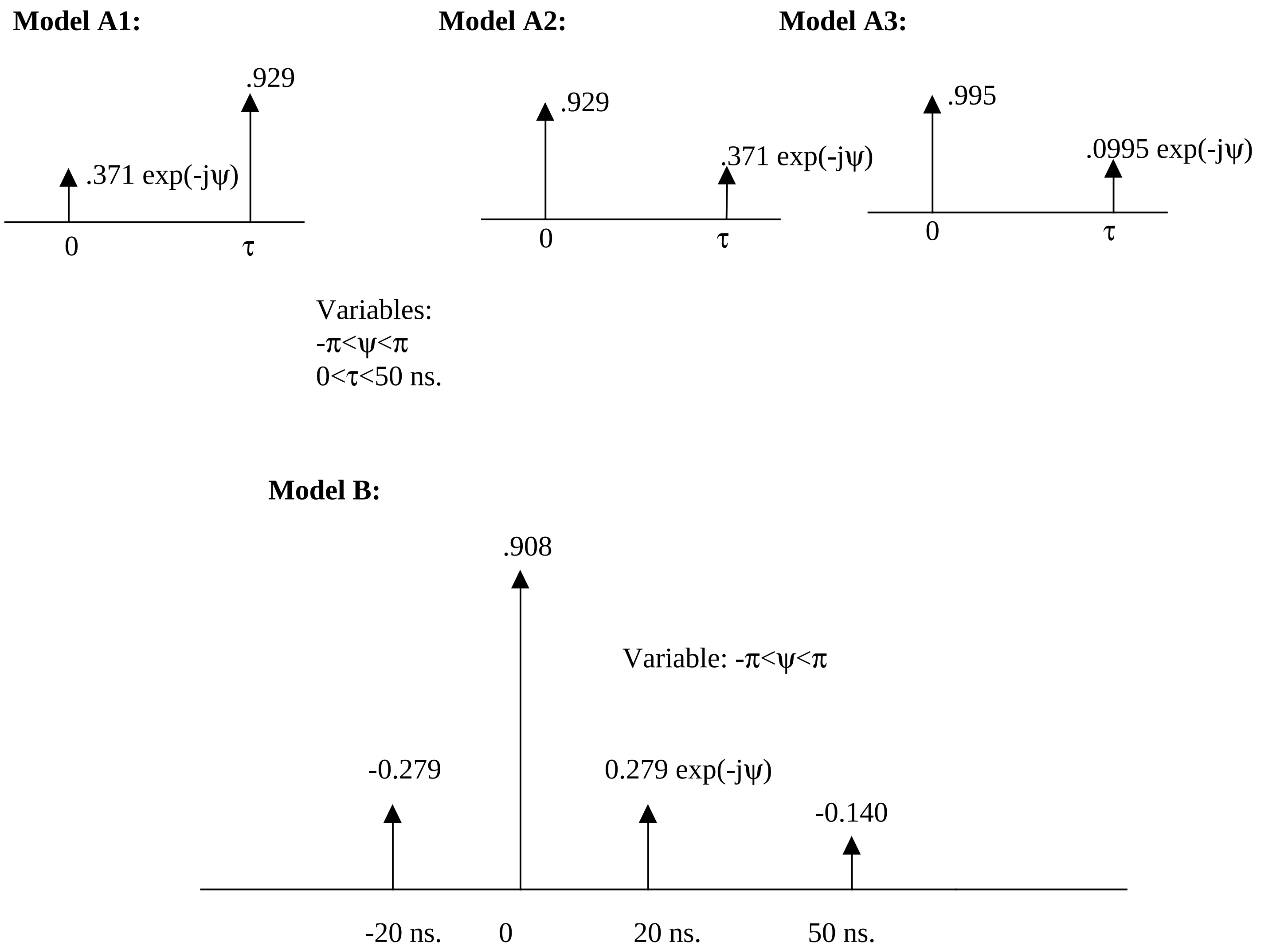

Fig. M3 Proposed multipath models

Models A1, A2 and A3 are 2-ray models, with variable parameters τ and ψ. These control the location and depth of the single notch in the frequency domain. Their relative echo magnitude is lower than that in the ETSI/BRAN models G3 and G4 in **Fig. M2**, but it should be noted that the service environment envisaged by the ETSI/BRAN Hiperaccess standards group may encounter worse multipath, including residential customers who may not have clear line of sight. A3 is least severe, since its echo component, at –20dB relative to the main echo, is relatively small. Model B is reminiscent, but somewhat more severe than the worst Kanata responses of **Fig. M1**, but is much less severe than the worst Parkwood Hills responses [Fal99b]. Typical frequency responses for several values of τ and ψ are shown in **Fig. M4.**

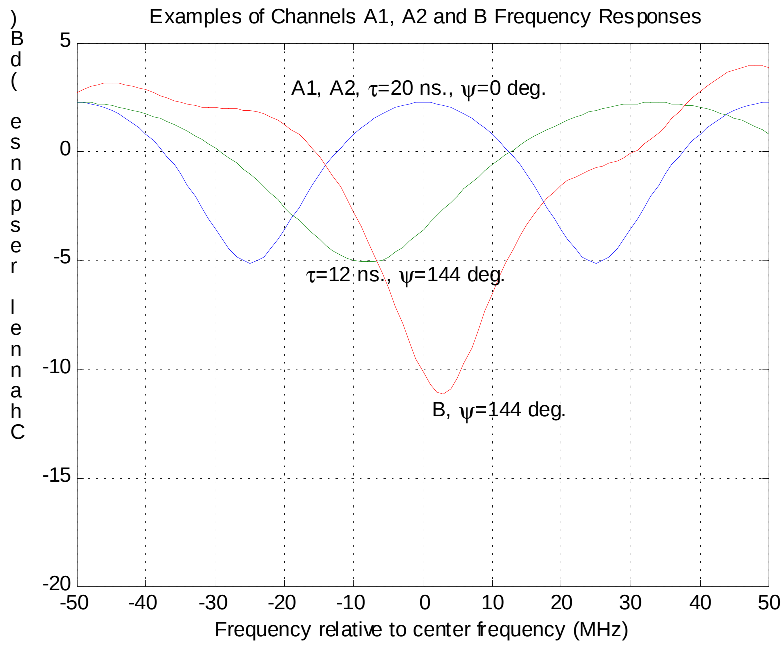

Fig. M4 Frequency responses of channel models A1, A2 and B

A receiver with no adaptive equalizer, but with appropriate error correction coding should be able to cope with channel A3, but would have difficulty with A1, A2 and B. For unequalized QPSK systems with τ=symbol period, $\psi=\pm 135°$ would move the intersymbol interference component closest to the receiver's decision boundary, and hence would give the highest bit error rate in these responses. Models A2 and A3 would be easily handled by a simple equalizer such as a DFE (decision feedback equalizer), with a few forward taps and one feedback tap, or by a simple Viterbi equalizer. Because of its "non-causal" nature, Model A1 would require a DFE with more forward taps. Examples of the performance of a fractional-spaced decision feedback equalizer with 8 forward and 1 feedback tap coefficient are given in **Table 1**, as functions of symbol rate and phase angle ψ for Models A1, A2 and B. The echo delay τ is assumed to be 20 ns. The signal to thermal noise ratio is 30 dB[1], and 25% rolloff square root raised cosine filters are assumed at the transmitter and receiver. The performance metric here is the degradation of the output equalizer's signal to noise ratio relative to the case of an ideal channel with no multipath echoes. For example if the input SNR is 30 dB, a degradation of 5 dB means the SNR at the equalizer's output due to multipath is 25 dB.

[1] A high SNR value of 30 dB was chosen for illustration purposes, to emphasize differences due to different multipath conditions.

Degradation in output SNR relative to noise-only case (dB)				
Symbol rate (Ms/s.)	**ψ (degrees)**	**Model A1**	**Model A2**	**Model B**
50	0	1.0	0.6	3.5
50	±45	3.1	0.6	5.1
50	±90	4.5	0.6	6.4
50	±135	4.7	0.6	5.5
50	±180	4.5	0.6	4.8
25	0	-1.4	-1.4	0.2
25	±45	-0.8	-0.8	0.8
25	±90	1.0	0.8	2.3
25	±135	2.8	2.3	4.5
25	±180	3.5	2.8	5.8

Table 1. (8,1) fractional-spaced DFE output mean squared error relative to noise-only case for the Models A1,A2 and B.

Note the relatively larger degradations for Model B. Note too that for each model at the lower symbol rate, phase shifts ψ approaching 180° produce partial signal cancellation (a manifestation of a fade), resulting in greater SNR degradation. These performance results are offered for illustration only; they do not necessarily represent typical system operating conditions or design. Better performance with more efficient adaptive equalizer structures may be available by use of more tap coefficients, symbol timing optimization, different rolloff factors, maximum likelihood sequence estimation in place of the DFE, etc. [Fal99a] shows equalizer performance over the same range of Kanata and Parkwood Hills channels described in [Fal99b].

4c. Time Variability

There is relatively little measurement data on time variations of fixed broadband millimeter wave radio links [Pap97b]. However measurements of fading bandwidths due to foliage movement reported in [Naz99] suggest that a typical worst case fading bandwidth for the amplitude of a 30 GHz carrier could be up to about 200 Hz. This would correspond to a maximum Doppler shift arising from movement of about 2 m./s. We know of no data on time variation of the phase of multipath components. In any case it seems clear that time variation will be extremely slow relative to envisaged bit rates (e.g. one cycle of 200 Hz Doppler spans 10^4 bit intervals at 2

Mb/s, and 10^5 bit intervals at 20 Mb/s. Therefore specification of a precise model of time variability of multipath seems unnecessary.

5. Acknowledgements

It is a pleasure to acknowledge the discussions and help of Naftali Chayat, Bruce Cochran, Scott Enserink, Lucille Rouault, Val Rhodes and Benoit Verbaere.

6. References

[Cha00] N. Chayat, “Some Models for Comparing PHY Proposals”, IEEE802.16pc-00/nn, Jan. 12, 2000

[Erc99] V. Erceg, D.G. Michelson, S.S. Ghassemzadeh, L.J. Greenstein, A.J. Rustako, P.B. Guerlain, M.K. Dennison , R.S. Roman, D.J. Barnickel, S.C. Wang and R.R. Miller, “A Model for the Multipath Delay Profile of Fixed Wireless Channels”, IEEE J. Sel. Areas in Communications, Vol. 17, No. 3, March, 1999, pp. 399-410.

[ETSI99] ETSI/BRAN document HAPHY151TL03**,** “Channel model suitable for bands over 20 GHz”, 21 Sept. 1999.

[Fal99a] D. Falconer and R. Saini, IEEE 802.16pc-99/28, “Equalization Requirements for Millimeter Wave Fixed Broadband Wireless Access Systems” Aug. 18, 1999.

[Fal99b] D. Falconer, IEEE802.16pc-00/01, “Multipath Measurements and Modelling for Fixed Broadband Wireless Systems in aResidential environment”, Dec. 20, 1999.

[Hon97] M. Honkanen and S-G Haffman, “New Aspects on Nonlinear Power Amplifier Modeling in Radio Communication System Simulations”, Proceedings of the IEEE International Symposium on Personal, Indoor, and Mobile Communications, PIMRC 1997, Helsinki, Finland, pp. 844-848, Sep. 1-4, 1997.

[Kay72], A.R. Kaye, D.A. George, and M.J. Eric, “Analysis and compensation of bandpass nonlinearities for communications,” IEEE Trans. Communications Technology, vol. COM-20, pp.965-972, October 1972.

[Pap97a] P.B. Papazian, G.A. Hufford, R.J. Achatz and R. Hoffman, “Study of the Local Multipoint Distribution Service Radio Channel”, IEEE Trans. Broadcasting, Vol. 43, No. 2, June, 1997, pp. 175-184.

[Pap97b] P.B. Papazian and G.A. Hufford, “Time Variability and Depolarization of the Local Multipoint Distribution Service Radio Channel”, Proc. 1997 Wireless Communications Conf., Boulder, CO, Aug. 1997.

[Naz99] N. Naz, “Temporal Variation Characterization for LMCS Channel and System design Implications”, M.Eng thesis, dept. of systems and Computer Engineering, Carleton University, Ottawa, Canada, May 1999. Also: N. Naz and D.D. Falconer, “Temporal Variations Characterization for Fixed wireless at 29.5 GHz”, to be presented at VTC2000, Tokyo, May, 2000.

[Rap91] C. Rapp, “Effects of HPA-Nonlinearity on an 4-DPSK/OFDM-Signal for a Digital Sound Broadcasting System,” Proc. 2nd European Conf. On Satellite Communications, Liege,Belgium, pp. 176-184, October 22-24, 1991.

[Sal81] A.A.M. Saleh, “Frequency-independent and frequency-dependent nonlinear models of TWT amplifiers,” IEEE Trans. Communications, vol. COM-29, pp.1715-1720, November 1981.

[Vio88] E.J. Violette, R.H. Espeland, R.O. DeBolt and F. Schwering, “Millimeter-Wave Propagation at Street Level in an Urban Environment”, IEEE Trans. Geoscience and Remote Sensing, Vol. 26, No. 3, May, 1988, pp. 368-380.

[Xu99] H. Xu, T.S. Rappaport, R.J. Boyle, And J.H. Schaffner, “38 GHz Wideband Point-to-Multipoint Radio Wave Propagation Study for a Campus Environment”, Proc. IEEE VTC ’99, Houston, May 1999.